Eidgenössische Technische Hochschule Zürich
Ecole polytechnique fédérale de Zurich
Politecnico federale di Zurigo
Swiss Federal Institute of Technology Zurich

Convergence analysis of an adaptive finite element method for distributed flux reconstruction

J. Li*, M. Li† and S. Mao

Research Report No. 2011-62
October 2011

Seminar für Angewandte Mathematik
Eidgenössische Technische Hochschule
CH-8092 Zürich
Switzerland

*Shenzhen Institutes of Advanced Technology, Shenzhen, China
†School of Information Engineering, China University of Geosciences, Beijing, China

Convergence analysis of An Adaptive Finite Element Method for Distributed Flux Reconstruction

J. Li [*], M. Li [†] S. Mao [‡]

Abstract

This paper studies convergence analysis of an adaptive finite element algorithm for numerical estimation of some unknown distributed flux in a stationary heat conduction system, namely recovering the unknown Neumann data on interior inaccessible boundary using Dirichlet measurement data on outer accessible boundary. Besides global upper and lower bounds established in [23], a posteriori local upper bounds and quasi-orthogonality results concerning the discretization errors of the state and adjoint variables are derived. Convergence and quasi-optimality of the proposed adaptive algorithm are rigorously proved. Numerical results are presented to illustrate the quasi-optimality of the proposed algorithm.

Key Words: Inverse problems, adaptive finite element method, a posteriori error estimates, quasi-orthogonality, convergence analysis

AMS subject classification 2000: Primary 65N21; Secondary 65N50, 65N30

1 Introduction

In this paper we study convergence analysis of an adaptive finite element algorithm for numerical estimation of some unknown distributed flux in a stationary heat conduction system, namely recovering the unknown Neumann data, called *fluxes* in the sequel, on the interior inaccessible boundary using Dirichlet measurement data on the outer accessible boundary.

In heat conduction, the flux distribution is of paramount practical interest, e.g., the real-time monitoring in steel industry [1], the visualization by liquid crystal thermography [18], and estimating the freezing front velocity in the solidification process [36]. But its accurate distribution is rather difficult to obtain on some inaccessible boundary, such as the interior boundary of nuclear reactors and steel furnaces. Engineers seek to estimate them from accessible outer boundary measurements, which naturally gives rise to the inverse problem of estimating the distribution of fluxes. This inverse problem is essentially lack of continuous dependance on data, thus ill-posed in Hadamard's sense [22].

Numerous numerical investigations have been made for this distributed flux reconstruction problem, among which the least-squares formulation [35–37] has received intensive investigations and it has been implemented by means of the boundary integral method [37] and the finite element method [35]. Recently, adaptive techniques are introduced for this problem for efficiency consideration [23]. Guided by the a posteriori error estimates, the adaptive algorithm in [23] automatically refines the mesh to better approximate the local but potentially very important features of the distributed flux, e.g.,

[*]Shenzhen Institutes of Advanced Technology, Shenzhen, PR China (jz.li@siat.ac.cn).
[†]School of Information Engineering, China University of Geosciences, Beijing, 100083, PR China (limx@cugb.edu.cn)
[‡]SAM, Department of Mathematics, ETH Zürich, CH-8092 Zürich, Switzerland (shipeng.mao@sam.math.ethz.ch).

non-smooth boundaries, discontinuous fluxes, or singular fluxes with spikes or abrupt sign changes. The computational cost of the adaptive algorithm is significantly reduced, compared with that of the uniform refinement.

The research on Adaptive Finite Element Methods (AFEMs) dates back to the seminal work [2] in the late 1970s. The main themes in AFEMs is how to measure, control and effectively minimize the discretization error of quantities of interest based on the computed solution and given data, among which the difficulties lies in 1) deriving a posteriori error estimates and 2) proving convergence of the resulting adaptive algorithm based on those a posteriori error estimates.

AFEMs have witnessed significant advance in reducing the computational complexity and improving efficiency in the solution of a variety of partial differential equations in the past decades. In inverse problems and control community, adaptive methods have been applied with emphasis on deriving a posteriori error estimates, to mention a few: 1) the dual weighted residual framework in terms of some quantity of interest [3, 4, 9], which provides a general recipe to construct a posteriori error estimates; 2) adaptive parameter identification in elliptic systems [20]; 3) adaptive methods in PDE-constrained optimal control problems [25–27].

On the other hand, theoretical convergence analysis of adaptive finite element methods has made important progress in recent years. It started with Dörfler [19], who introduced a crucial marking strategy, from now on called Dörfler's marking strategy, and proved the strict energy reduction property for the Laplace equation provided the initial mesh satisfies the fineness assumption. Some breakthrough has been made on the optimality of adaptive finite element methods since the pioneering work of Binev, Dahmen, DeVore [10] and Stevenson [33]. In fact, the question of convergence and optimality of adaptive finite element methods has been subject to intensive studies in recent years, which is reflected from vast literature, see, e.g., [5–7, 12–15, 28, 30, 31]. However, most references aforementioned focused on direct model problems, as opposed to few literatures on inverse problems or optimal control problems arising from practice. Recently, Gaevskaya et al proved in [21] the first convergence result of AFEM for a simple optimal control problem by introducing the concept of data oscillation and the interior node property. By relaxing the interior node restriction, Becker and Mao [8] showed the convergence of AFEM by an alternative approach using a different marking strategy.

This paper is a subsequent one following [23]. In this work, based on the a posteriori error estimates derived in [23], we prove the convergence and quasi-optimality of a modified adaptive algorithm by using Dörfler's collective marking strategy, compared with that in [23]. The main ingredients for the analysis of the adaptive algorithm include a novel a posteriori *local* upper bounds and a pair of important quasi-orthogonality results concerning the discretization errors of the state and adjoint variables. Combined with global upper and lower bounds established in [23], convergence and quasi-optimality are rigorously proved for the proposed adaptive algorithm.

The paper is organized as follows. In section 2, we briefly formulate our flux reconstruction problem into a least-squares problem combined with Tikhonov regularization. Then the finite element discretization on a single grid is described. In Section 3, we introduce relevant terms of a posteriori error estimates and present an adaptive reconstruction algorithm under investigation. In Section 4, we prepare some important technical tools, including a posteriori local upper bound and two quasi-orthogonality results. In Section 5, we prove the convergence of the adaptive algorithm by showing the error reduction property of some total error measure, namely the discretization error plus the error estimator up to some positive constant. In Section 6, quasi-optimality of the adaptive algorithm is proved rigorously. In Section 7, numerical results are presented to verify the theoretical results.

Before ending this section, let's recall some notations and conventions throughout the paper. We adopt the standard notation $W^{m,p}(D)$ for Sobolev spaces on an open bounded domain D in $\mathbb{R}^2$, and write $H^m(D) = W^{m,2}(D)$ for $p = 2$. The norm and semi-norm of $H^m(D)$ are denoted respectively by $\|\cdot\|_{m,D}$ and $|\cdot|_{m,D}$. We use $(\cdot,\cdot)_D$ to denote the inner product in $L^2(D)$. When no confusion is

caused, we may simply drop D in the notation $\|\cdot\|_{m,D}$ and $(\cdot,\cdot)_D$. In addition, we will often use c or C to denote generic positive constants which are independent of mesh size h and functions involved.

2 Inverse problem and discretization

We briefly present in this section the mathematical formulation of the problem of flux distribution reconstruction, and its finite element discretization.

2.1 Mathematical formulation

Let Ω be an open and bounded domain in $\mathbb{R}^2$ with some smooth boundary Γ consisting of two disjointed parts, namely $\Gamma = \Gamma_a \cup \Gamma_i$. The boundaries Γ_i and Γ_a refer to the part of the boundary Γ that is inaccessible and accessible to experimental measurement, respectively. The steady-state heat conduction problem could be described by the elliptic PDE:

$$\begin{cases} -\nabla\cdot(\alpha(x)\nabla u(x)) = f(x), \ x\in\Omega, \\ \alpha(x)\dfrac{\partial u}{\partial n} + k(u(x)-u_a(x)) = 0, \ x\in\Gamma_a, \\ \alpha(x)\dfrac{\partial u}{\partial n} + q(x) = 0, \ x\in\Gamma_i, \end{cases} \tag{2.1}$$

where the given data include the source f, the ambient temperature u_a, the heat transfer coefficient k and the heat conductivity α. The flux $q(x)$ on Γ_i is the quantity of interest in this work.

The inverse problem that we are interested in is to recover the distributed flux $q(x)$ on the interior inaccessible part Γ_i, given the partial measurement data $z(x)$ of temperature $u(x)$ on the outer accessible part Γ_a.

Due to the severe ill-posedness (see, e.g., [35, Theorem 2.2]), the reconstruction is carried out through the output least-squares formulation combined with the Tikhonov regularization. More precisely, we seek $q(x)$ by solving

$$\min_{q\in L^2(\Gamma_i)} J(q) = \frac{1}{2}\|u(q)-z\|^2_{0,\Gamma_a} + \frac{\beta}{2}\|q\|^2_{0,\Gamma_i}, \tag{2.2}$$

where $u(q): L^2(\Gamma_i)\to H^1(\Omega)$ represents the solution operator of the direct problem (2.1), which maps parameter q to solution u.

The necessary and sufficient optimality conditions of the regularized formulation (2.2) are characterized by the following theorem (cf. [23, Thm. 2.1]).

Lemma 2.1. *The optimization problem* (2.2) *admits a unique solution q. And q is the minimizer if and only if there is a costate $p\in H^1(\Omega)$ such that the triplet (u,p,q) satisfies the following optimality conditions:*

$$\begin{cases} (\alpha\nabla u,\nabla\phi) + (ku,\phi)_{\Gamma_a} = (f,\phi) + (ku_a,\phi)_{\Gamma_a} - (q,\phi)_{\Gamma_i}, & \forall\ \phi\in H^1(\Omega), \\ (\alpha\nabla p,\nabla v) + (kp,v)_{\Gamma_a} = (u-z,v)_{\Gamma_a}, & \forall\ v\in H^1(\Omega), \\ J'(q)(w) = (\beta q - p, w)_{\Gamma_i} = 0, & \forall\ w\in L^2(\Gamma_i). \end{cases} \tag{2.3}$$

2.2 Finite element discretization

In this subsection, we describe the finite element descritization of the continuous nonlinear optimization problem (2.1)–(2.2) on a single grid. Let T^h be a partition of Ω into disjoint open regular triangles τ so that $\bar\Omega = \cup_{\tau\in T^h}\bar\tau$ in the sense of [16]. The natural restriction of T^h on the boundary of Ω forms

the triangulations of Γ_i and Γ_a, denoted by Γ_i^h and Γ_a^h, respectively. Let F^h be the set of all edges of the triangulation T^h and F_0^h be the set of all faces which are not on the boundary of Ω, namely, $F^h = F_0^h \bigcup(\Gamma_i^h \cup \Gamma_a^h)$. Associated with T^h is the piecewise linear finite element subspace V^h of $C(\bar{\Omega})$. And we take the feasible approximation space for parameters q to be the natural restriction of V^h on the boundary Γ_i, denoted by $V_{\Gamma_i}^h$.

Then the discrete counterpart of the continuous problem (2.2) can be formulated as:

$$\min_{q_h \in V_{\Gamma_i}^h} J_h(q_h) = \frac{1}{2}\|u_h(q_h) - z\|_{0,\Gamma_a}^2 + \frac{\beta}{2}\|q_h\|_{0,\Gamma_i}^2, \tag{2.4}$$

where $u_h(q_h) \in V^h$ is the finite element solution of (2.1) with the discrete flux q_h, namely

$$(\alpha\nabla u_h, \nabla\phi_h) + (ku_h, \phi_h)_{\Gamma_a} = (f, \phi_h) + (ku_a, \phi_h)_{\Gamma_a} - (q_h, \phi_h)_{\Gamma_i}, \quad \forall \phi_h \in V^h. \tag{2.5}$$

As in Lemma 2.1, the discrete optimality conditions can be obtained by simply replacing (u, p, q) with (u_h, p_h, q_h) and continuous spaces with finite element spaces (cf. [23, Eq. (2.6)]).

$$\begin{cases} (\alpha\nabla u_h, \nabla\phi_h) + (ku_h, \phi_h)_{\Gamma_a} = (f, \phi_h) + (ku_a, \phi_h)_{\Gamma_a} - (q_h, \phi_h)_{\Gamma_i}, & \forall\ \phi_h \in V^h, \\ (\alpha\nabla p_h, \nabla\phi_h) + (kp_h, \phi_h)_{\Gamma_a} = (u_h - z, \phi_h)_{\Gamma_a}, & \forall\ \phi_h \in V^h, \\ J_h'(q_h)(w_h) = (\beta q_h - p_h, w_h) = 0, & \forall\ w_h \in V_{\Gamma_i}^h. \end{cases} \tag{2.6}$$

We define the energy norm by

$$|||\cdot|||_e^2 = (\alpha\nabla\cdot, \nabla\cdot) + (k\cdot, \cdot)_{\Gamma_a},$$

which is equivalent to the H^1-nrom $\|\cdot\|_1$ by the Poincaré inequality.

The following lemma concerning the a priori L^2 error estimate is very crucial in the subsequent convergence analysis. Since its proof is rather technical and beyond the scope in this paper, we omit its details and refer interested readers to [24, Theorem 3.2].

Lemma 2.2. *Let (u, p, q) and (u_h, p_h, q_h) be the solutions of (2.3) and (2.6), respectively. Then there exists a constant $C_0 > 0$ depending only on the minimum angle of T^h such that*

$$\|u - u_h\|_0^2 + \|p - p_h\|_0^2 \ \leq\ C_0 h^{2\gamma}(|||u - u_h|||_e^2 + |||p - p_h|||_e^2), \tag{2.7}$$

with the constant $\gamma \in (0, 1]$ depending on the geometry of the domain.

3 Adaptive algorithm

In this section, we present our adaptive algorithm in detail. A posteriori error estimates derived in [23] will be recalled, and Döfler's collective marking strategy is used to replace the old one.

First of all, we introduce some notations to be used in the sequel. Let $h_\tau = |\tau|^{\frac{1}{2}}$ denote the size of the element τ in T^h, and $h_l = |l|$ the size of the edge l in F^h. We denote by Ω_l the union of two elements in T^h sharing l. In addition, we denote by $N_{\mathcal{F}}$ the cardinal number of a finite set $\mathcal{F}$. In particular, for a sequence of successively refined regular meshes $\{T^k\}_{k\geq 0}$ with edge set $\{F^k\}_{k\geq 0}$. In the sequel, N_{T^k}, the number of degrees of freedom on T^k, is abbreviated by N_k

A typical adaptive finite element method through local refinement can be written as the following loop:

$$\textbf{SOLVE} \rightarrow \textbf{ESTIMATE} \rightarrow \textbf{MARK} \rightarrow \textbf{REFINE}.$$

In this section, we shall focus on the modules **Estimate** and **Mark**

The step **Estimate** consists of deriving the residual-type a posteriori error estimator, which can be found in [23]. We first introduce the following error estimator terms, which consists of some volume and edge residuals:

$$\begin{cases} \eta_{1,h}^2(\tau) = h_\tau^2 \int_\tau (|\nabla \cdot (\alpha \nabla p_h)|^2 + |\nabla \cdot (\alpha \nabla u_h) + f|^2) dx, & \forall\ \tau \in T^h, \\ \eta_{2,h}^2(l) = h_l \int_l ([(\alpha \nabla p_h) \cdot n]_l^2 + [(\alpha \nabla u_h) \cdot n]_l^2) ds, & \forall\ l \in F^h, \end{cases} \tag{3.8}$$

where $[\,\cdot\,]$ stands for the jump of the concerned quantity across the interior edge l of adjacent elements, and for boundary edges, it is defined as follows:

$$[(\alpha \nabla p_h) \cdot n]_l = \begin{cases} \alpha \dfrac{\partial p_h}{\partial n} + k p_h - u_h + z, & \forall\ l \in F_a^h, \\ \alpha \dfrac{\partial p_h}{\partial n}, & \forall\ l \in F_i^h, \end{cases} \tag{3.9}$$

$$[(\alpha \nabla u_h) \cdot n]_l = \begin{cases} \alpha \dfrac{\partial u_h}{\partial n} + k u_h - k u_a, & \forall\ l \in F_a^h, \\ \alpha \dfrac{\partial u_h}{\partial n} + q_h, & \forall\ l \in F_i^h. \end{cases} \tag{3.10}$$

In the subsequent analysis, we also need to treat the oscillation terms

$$\begin{cases} \mathrm{osc}_{1,h}^2(u_h, p_h, \tau) = h_\tau^2 (\|\nabla \cdot (\alpha \nabla p_h) - \overline{\nabla \cdot (\alpha \nabla p_h)}\|_{0,\tau}^2 \\ \qquad\qquad + \|\nabla \cdot (\alpha \nabla u_h) + f - \overline{\nabla \cdot (\alpha \nabla u_h) + f}\|_{0,\tau}^2), & \forall\ \tau \in T^h, \\ \mathrm{osc}_{2,h}^2(u_h, p_h, l) = h_l (\|[(\alpha \nabla u_h) \cdot n]_l - \overline{[(\alpha \nabla u_h) \cdot n]_l}\|_{0,l}^2 \\ \qquad\qquad + \|[(\alpha \nabla p_h) \cdot n]_l - \overline{[(\alpha \nabla p_h) \cdot n]_l}\|_{0,l}^2), & \forall\ l \in F^h, \end{cases} \tag{3.11}$$

where $\overline{\cdot}$ denotes the average of the corresponding quantities in the associated elements or edges. Note that these oscillation terms are only used in theoretical analysis, but not computed in practice.

By noticing the relationships $\beta q = p$, and $\beta q_h = p_h$ through (2.3) and (2.6). The estimates of $q - q_h$ and $p - p_h$ are linearly dependent, therefore we choose to estimate $p - p_h$. This key observation facilitate the subsequent convergence analysis.

For any subset $\mathcal{F} \subset F^h$, we define

$$\mathcal{M}_{\mathcal{F}} := \sum_{l \in \mathcal{F}} \sum_{\tau \in \Omega_l} \tau \tag{3.12}$$

and

$$\eta_h^2(\mathcal{F}) := \sum_{\tau \in \mathcal{M}_{\mathcal{F}}} \eta_{1,h}^2(\tau) + \sum_{l \in \mathcal{F}} \eta_{2,h}^2(l), \tag{3.13}$$

$$\mathrm{osc}_h^2(u_h, p_h, \mathcal{F}) := \sum_{\tau \in \mathcal{M}_{\mathcal{F}}} \mathrm{osc}_{1,h}^2(u_h, p_h, \tau) + \sum_{l \in \mathcal{F}} \mathrm{osc}_{2,h}^2(u_h, p_h, l). \tag{3.14}$$

For brevity, we drop F^h when $\mathcal{F} = F^h$ when no confusion is caused.

When $\{T^k\}_{k \geq 0}$ are considered, the subscript h in u_h, q_h, and (3.8)–(3.14) is always replaced by k to denote the terms associated with the specific mesh T^k.

As for the **Refine** step, the refinement rule for dividing the marked triangles has to been chosen to meet two requirements: i) The family of meshes obtained by this rule is conforming and shape regular; ii) The number of elements added can be controlled to ensure the overall optimality of the refinement procedure.

In this article, we define the family of admissible meshes in the following recursive way. Starting from an initial mesh T^0, we denote by $\mathcal{R}loc(T^H, \mathcal{F})$ with $\mathcal{F} \subset F_H$ the mesh resulting from a local mesh refinement algorithm such as the newest vertex bisection algorithm, see [10, 29] for details. We first recall the following property of the newest vertex bisection.

Lemma 3.1. *Assume that the initial mesh T^0 verifies condition (b) of section 4 in [34]. Let $T^k, k = 0, \ldots n$ be a sequence of locally refined meshes generated by the newest vertex bisection, starting from the initial mesh T^0. Let $\mathcal{F}^k \subset F^k, k = 0, \ldots n-1$ be the collection of all marked edges in step k. Then T^k, $k = 0, 1, \ldots$, are uniformly shape regular and the shape regularity of T^k, $k = 0, 1, \ldots$, only depends on that of T^0. Furthermore, we have*

$$N_n \leq N_0 + C_0^* \sum_{k=0}^{n-1} N_{\mathcal{F}^k}. \tag{3.15}$$

Lemma 3.1 and the complexity estimate (3.15) are known to be true for the newest vertex bisection algorithm, see [10, 34] (where the set of marked cells instead of the set of marked edges is used).

The adaptive finite element algorithm for our inverse problem is described in the following:

Algorithm 1 $\mathcal{AFEM}$

(0) Choose parameter $\theta \in (0, 1]$, and an initial mesh T^0, and set $k = 0$.

(1) Solve the discrete optimization problem (2.6) on T^k to obtain the finite element solutions (u_k, p_k, q_k).

(2) Compute the error estimator $\eta_k(l)$ for each edge $l \in F^k$.

(3) Mark a subset $\mathcal{F}^k \subset F^k$ with minimal cardinality such that

$$\eta_k^2(\mathcal{F}^k) \geq \theta\, \eta_k^2, \tag{3.16}$$

where for abbreviation we write $\eta_k^2 := \eta_{h_k}^2(F^k)$ on T^k.

(4) Refine the current mesh to get a new mesh, i.e., $T^{k+1} := \mathcal{R}loc(T^k, \mathcal{F}^k)$.

(5) Set $k := k + 1$ and go to step (1).

4 A posteriori error estimates and some lower and upper bounds

In this section we present a posteriori error estimates for the finite element approximation (2.4)–(2.5) for our inverse problem, and prove a new a posteriori local upper bounds and two quasi-orthogonality results, which will play key roles in the subsequent convergence and optimality analysis of our adaptive FEM algorithm. Let's first recall the following lemmas concerning the global upper and lower bounds of the discretization error derived in [23].

Lemma 4.1. *[23, Thm. 3.5] Let (u, p, q) and (u_h, p_h, q_h) be the solutions of (2.3) and (2.6), respectively. Then there exists a constant $C_1 > 0$ depending only on the minimum angle of T_h such that*

$$|||u - u_h|||_e^2 + |||p - p_h|||_e^2 \;\leq\; C_1 \eta_h^2. \tag{4.1}$$

Lemma 4.2. *[23, Thm. 3.9] Let (u, p, q) and (u_h, p_h, q_h) be the solutions of (2.3) and (2.6), respectively. Then there exists a constant $C_2 > 0$ depending only on the minimum angle of T^h such that*

$$\eta_h^2 \leq C_2(|||u - u_h|||_e^2 + |||p - p_h|||_e^2 + osc_h^2(u_h, p_h)). \tag{4.2}$$

The following lemma establishes the error reduction property between two nested meshes.

Lemma 4.3. *Let T^h, T^H be two nested meshes with $T^H \subset T^h$ and $\mathcal{F} = F^H \backslash (F^H \cap F^h) \subset F^H$. Let (u_H, p_H, q_H) and (u_h, p_h, q_h) be the solutions to (2.6) on meshes T^h and T^H, respectively. Then there exists a constant $C_3 > 0$ and C_3^* depending only on the minimum angle of T^H and a parameter $0 < \delta_1 < 1$ such that*

$$\eta_h^2 \leq (1+\delta_1)\eta_H^2 - \frac{1+\delta_1}{2}\eta_H^2(\mathcal{F}) + C_3(1+\frac{1}{\delta_1})(|||u_H - u_h|||_e^2 + |||p_H - p_h|||_e^2), \tag{4.3}$$

and

$$osc_H^2(u_H, p_H, F^H \cap F^h) - 2osc_h^2(u_h, p_h, F^H \cap F^h) \leq C_3^*(|||u_H - u_h|||_e^2 + |||p_H - p_h|||_e^2). \tag{4.4}$$

Proof. The proof of the first and second inequalities can follow the similar lines in the proof of Corollary 3.4 and Corollary 3.5 in [14], respectively. We omit it here for brevity. □

Compared with the global upper bounds in Lemma 4.1, the following lemma presents a novel a posteriori local upper bounds by the estimators on the marked sets.

Lemma 4.4. *Let T^h, T^H be two nested meshes with $T^H \subset T^h$ and $\mathcal{F} = F^H \backslash (F^H \cap F^h) \subset F^H$. Let (u_H, p_H, q_H) and (u_h, p_h, q_h) be the solutions to (2.6) on meshes T^H and T^h, respectively. There exists a constant $C_4 > 0$ depending only on the minimum angle of T^H such that*

$$|||u_H - u_h|||_e^2 + |||p_H - p_h|||_e^2 \leq C_4\big(\eta_H^2(\mathcal{F}) + H^{2\gamma}(|||u - u_H|||_e^2 + |||p - p_H|||_e^2)\big), \tag{4.5}$$

and

$$\#\mathcal{F} \leq C_5\,(N_h - N_H). \tag{4.6}$$

Proof. We first bound the term $|||u_H - u_h|||_e$. Let I_H be the Scott-Zhang quasi-interpolation operator defined on mesh T^H (cf. [32]), which satisfies

$$\|v - I_H v\|_{s,\tau} \leq C \sum_{\bar{\tau}\cap\bar{\tau}'\neq\emptyset} H_\tau^{1-s}|v|_{1,\tau'} \quad \forall\, \tau \in T^H. \tag{4.7}$$

Then by the first equation of (2.6) over mesh T^h and T^H, and by integrating by parts in each element and applying the Cauchy-Schwartz inequality, we obtain

$$\begin{aligned}
|||u_h - u_H|||_e^2 &\leq \big(\alpha\nabla(u_h - u_H), \nabla(u_h - u_H)\big) + \big(k(u_h - u_H), u_h - u_H\big)_{\Gamma_a} \\
&\overset{(2.6)}{=} \big(f, u_h - u_H\big) + \big(ku_a, u_h - u_H\big)_{\Gamma_a} - \big(q_h, u_h - u_H\big)_{\Gamma_i} \\
&\quad -\big(\alpha\nabla u_H, \nabla(u_h - u_H)\big) + \big(ku_H, u_h - u_H\big)_{\Gamma_a} \\
&= \big(f, u_h - u_H\big) + \big(ku_a, u_h - u_H\big)_{\Gamma_a} - \big(q_h, u_h - u_H\big)_{\Gamma_i} \\
&\quad -\big(\alpha\nabla u_H, \nabla I_H(u_h - u_H)\big) + \big(ku_H, I_H(u_h - u_H)\big)_{\Gamma_a} \\
&\quad +\Big(\alpha\nabla u_H, \nabla\big(I_H(u_h - u_H) - (u_h - u_H)\big)\Big) \\
&\quad +\big(ku_H, I_H(u_h - u_H) - (u_h - u_H)\big)_{\Gamma_a} \\
&\overset{(2.6)}{=} \big(f, u_h - u_H - I_H(u_h - u_H)\big) - \big(q_h - q_H, u_h - u_H\big)_{\Gamma_i} \\
&\quad + \sum_{l\in\Gamma_i^H}\int_l \big((\alpha\nabla u_H)\cdot n + ku_H - ku_a\big)\big(I_H(u_h - u_H) - (u_h - u_H)\big)ds
\end{aligned}$$

$$
\begin{aligned}
&+\sum_{l\in\Gamma_a^H}\int_l\big((\alpha\nabla u_H)\cdot n+q_H\big)\big(I_H(u_h-u_H)-(u_h-u_H)\big)ds \qquad (4.8)\\
&\quad+\sum_{\tau\in T^H}\int_\tau\big(\nabla\cdot(\alpha\nabla p_h)\big)\big(u_h-u_H-I_H(u_h-u_H)\big)dx\\
&\quad-\sum_{l\in F_0^H}\int_l[(\alpha\nabla u_H)\cdot n]_l\big(u_h-u_H-I_H(u_h-u_H)\big)ds\\
&=\sum_{\tau\in\mathcal{M}_\mathcal{F}}\int_\tau\big(f+\nabla\cdot(\alpha\nabla u_H)\big)\big(u_h-u_H-I_H(u_h-u_H)\big)dx\\
&\quad-\sum_{l\in\mathcal{F}}\int_l[(\alpha\nabla u_H)\cdot n]_l\big(u_h-u_H-I_H(u_h-u_H)\big)ds\\
&\qquad-\beta^{-1}\big(p_h-p_H,u_h-u_H\big)_{\Gamma_i}\\
&\overset{(4.7)}{\leq} C\left(\sum_{\tau\in\mathcal{M}_\mathcal{F}}\int_\tau|f+\nabla\cdot(\alpha\nabla u_H)|^2dx\right)^{\frac12}|||u_h-u_H|||_e\\
&\qquad+C\left(\sum_{l\in\mathcal{F}}\int_l[(\alpha\nabla u_H)\cdot n]_l^2ds\right)^{\frac12}|||u_h-u_H|||_e\\
&\qquad+C\|u_h-u_H\|_{0,\Gamma_i}\|p_h-p_H\|_{0,\Gamma_i}\\
&\leq C(\eta_H(\mathcal{F})|||u_h-u_H|||_e+\tfrac12\|u_h-u_H\|_{0,\Gamma_i}^2+\tfrac12\|p_h-p_H\|_{0,\Gamma_i}^2),
\end{aligned}
$$

where we have used the fact that $I_H(u_h-u_H)=u_h-u_H$ on the elements in the subset $T^h\cap T^H$.

We next bound the term $|||p_h-p_H|||_e$. By a similar argument, applying the the Poincaré inequality, the second equation of (2.6) over mesh T^h and T^H, and integrating by parts over each element and the Cauchy-Schwartz inequality, we derive

$$
\begin{aligned}
|||p_h - p_H|||_e^2 &\leq \big(\alpha\nabla(p_h - p_H), \nabla(p_h - p_H)\big) + \big(k(p_h - p_H), p_h - p_H\big)_{\Gamma_a} \\
&\overset{(2.6)}{=} \big(u_h - z, p_h - p_H\big)_{\Gamma_a} - \big(\alpha\nabla p_H, \nabla(p_h - p_H)\big) - \big(kp_H, p_h - p_H\big)_{\Gamma_a} \\
&= \big(u_h - z, p_h - p_H\big)_{\Gamma_a} - \big(\alpha\nabla p_H, \nabla I_H(p_h - p_H)\big) - \big(kp_H, I_H(p_h - p_H)\big)_{\Gamma_a} \\
&\quad -\Big(\alpha\nabla p_H, \nabla\big((p_h - p_H) - I_H(p_h - p_H)\big)\Big) \\
&\quad -\big(kp_H, p_h - p_H - I_H(p_h - p_H)\big)_{\Gamma_a} \\
&\overset{(2.6)}{=} \big(u_h - z, p_h - p_H\big)_{\Gamma_a} - \big(u_H - z, I_H(p_h - p_H)\big)_{\Gamma_a} \\
&\quad -\Big(\alpha\nabla p_H, \nabla\big((p_h - p_H) - I_H(p_h - p_H)\big)\Big) \\
&\quad -\big(kp_H, p_h - p_H - I_H(p_h - p_H)\big)_{\Gamma_a} \\
&= \big(u_h - u_H, p_h - p_H\big)_{\Gamma_a} \\
&\quad + \sum_{l\in\Gamma_a^H} \big(u_H - z - kp_H - (\alpha\nabla p_H)\cdot n\big)\big(p_h - p_H - I_H(p_h - p_H)\big)ds \\
&\quad - \sum_{l\in\Gamma_i^H} \int_l (\alpha\nabla p_H)\cdot n\big(p_h - p_H - I_H(p_h - p_H)\big)ds \\
&\quad - \sum_{l\in F_0^H} \int_l (\alpha\nabla p_H)\cdot n\big(p_h - p_H - I_H(p_h - p_H)\big)ds \\
&\quad - \sum_{\tau\in T^H} \int_\tau \nabla\cdot(\alpha\nabla p_H)\big((p_h - p_H) - I_H(p_h - p_H)\big)dx \\
&= \big(u_h - u_H, p_h - p_H\big)_{\Gamma_a} \\
&\quad - \sum_{\tau\in\mathcal{M}_\mathcal{F}} \int_\tau \nabla\cdot(\alpha\nabla p_H)\big((p_h - p_H) - I_H(p_h - p_H)\big)dx \\
&\quad + \sum_{l\in\mathcal{F}} \int_l [\alpha\nabla p_H)\cdot n]_l\big(p_h - p_H - I_H(p_h - p_H)\big)ds \\
&\overset{(4.7)}{\leq} C(\eta_H(\mathcal{F})|||p_h - p_H|||_e + \tfrac{1}{2}\|u_h - u_H\|_{0,\Gamma_a}^2 + \tfrac{1}{2}\|p_h - p_H\|_{0,\Gamma_a}^2).
\end{aligned} \tag{4.9}
$$

On the other hand, by the trace inequality, Young's inequality and Lemma 2.2, we get

$$
\begin{aligned}
\|u_h - u_H\|_{0,\Gamma}^2 &\leq c_1\|u_h - u_H\|_0\|u_h - u_H\|_1 \\
&\leq \tfrac{1}{C}\|u_h - u_H\|_1^2 + \tfrac{c_1 C}{4}\|u_h - u_H\|_0^2 \\
&\leq \tfrac{1}{C}\|u_h - u_H\|_1^2 + \tfrac{c_1 C}{2}(\|u - u_H\|_0^2 + \|u - u_h\|_0^2) \\
&\leq \tfrac{1}{C}\|u_h - u_H\|_1^2 + c_1 C\|u - u_H\|_0^2 \\
&\overset{(2.7)}{\leq} \tfrac{1}{C}\|u_h - u_H\|_1^2 + c_1 C C_0 H^{2\gamma}(|||u - u_H|||_e^2 + |||p - p_H|||_e^2).
\end{aligned} \tag{4.10}
$$

Similarly,

$$
\|p_h - p_H\|_{0,\Gamma}^2 \leq \frac{1}{C}\|p_h - p_H\|_1^2 + c_1 C C_0 H^{2\gamma}(|||u - u_H|||_e^2 + |||p - p_H|||_e^2). \tag{4.11}
$$

Then the desired result will be obtained by a collection of the above results together with a proper choice of the parameters of the Young's inequality. □

Finally we give an estimate for the quasi-orthogonality of the discretization error with respect to the energy norm, which explain the coupling relation of errors on two successive meshes.

Lemma 4.5. *Let T^h, T^H be two nested meshes with $T^H \subset T^h$ and $\mathcal{F} = F^H\backslash(F^H \cap F^h) \subset F^H$. Let (u_H, p_H, q_H) and (u_h, p_h, q_h) be the solutions to (2.6) on meshes T^h and T^H, respectively. Then there*

exists a constant $C_6 > 0$ depending on the minimum angle of T^H such that

$$\begin{aligned} |||u-u_h|||_e^2 + |||p-p_h|||_e^2 &\leq \tfrac{1+C_6H^\gamma}{1-2C_6H^\gamma}(|||u-u_H|||_e^2 + |||p-p_H|||_e^2) \\ &\quad -\tfrac{1-C_6H^\gamma}{1-2C_6H^\gamma}(|||u_h-u_H|||_e^2 + |||p_h-p_H|||_e^2). \end{aligned} \tag{4.12}$$

and

$$\begin{aligned} |||u-u_H|||_e^2 + |||p-p_H|||_e^2 &\leq \tfrac{1+2C_6H^\gamma}{1-C_6H^\gamma}(|||u-u_h|||_e^2 + |||p-p_h|||_e^2) \\ &\quad +\tfrac{1+C_6H^\gamma}{1-C_6H^\gamma}(|||u_h-u_H|||_e^2 + |||p_h-p_H|||_e^2). \end{aligned} \tag{4.13}$$

Proof. By the definition of the energy norm $|||\cdot|||_e$, the equations of (2.3) and (2.6), we derive

$$\begin{aligned} |||u-u_h|||_e^2 + |||p-p_h|||_e^2 &= \big(\alpha\nabla(u-u_h),\nabla(u-u_h)\big) + \big(k(u-u_h),u-u_h\big)_{\Gamma_a} \\ &\quad +\big(\alpha\nabla(p-p_h),\nabla(p-p_h)\big) + \big(k(p-p_h),p-p_h\big)_{\Gamma_a} \\ &= |||u-u_H|||_e^2 + |||p-p_H|||_e^2 - (|||u_h-u_H|||_e^2 + |||p_h-p_H|||_e^2) \\ &\quad +2\big(\alpha\nabla(u-u_h),\nabla(u_h-u_H)\big) + 2\big(k(u-u_h),u_h-u_H\big)_{\Gamma_a} \\ &\quad +2\big(\alpha\nabla(p-p_h),\nabla(p_h-p_H)\big) + 2\big(k(p-p_h),p_h-p_H\big)_{\Gamma_a} \\ &\overset{(2.3),(2.6)}{=} |||u-u_H|||_e^2 + |||p-p_H|||_e^2 - (|||u_h-u_H|||_e^2 + |||p_h-p_H|||_e^2) \\ &\quad +2(q-q_h,u_h-u_H)_{\Gamma_i} + 2(u-u_h,p_h-p_H)_{\Gamma_a} \\ &= |||u-u_H|||_e^2 + |||p-p_H|||_e^2 - (|||u_h-u_H|||_e^2 + |||p_h-p_H|||_e^2) \\ &\quad +2\beta^{-1}(p-p_h,u_h-u_H)_{\Gamma_i} + 2(u-u_h,p_h-p_H)_{\Gamma_a}, \end{aligned} \tag{4.14}$$

then by Cauchy-Schwarz inequality, the trace inequality, we have

$$\begin{aligned} &2\Big|\beta^{-1}(p-p_h,u_h-u_H)_{\Gamma_i} + (u-u_h,p_h-p_H)_{\Gamma_a}\Big| \\ \leq\ & c_2\big(\|p-p_h\|_{0,\Gamma}^2 + \|u-u_h\|_{0,\Gamma}^2\big) \\ &+c_2\big(\|u_h-u_H\|_{0,\Gamma}^2 + \|p_h-p_H\|_{0,\Gamma}^2\big) \\ \leq\ & c_2c_1\big(\|p-p_h\|_0\|p-p_h\|_1 + \|u-u_h\|_0\|u-u_h\|_1\big) \\ &+c_2c_1\big(\|u_h-u_H\|_0\|u_h-u_H\|_1 + \|p_h-p_H\|_0\|p_h-p_H\|_1\big) \\ \leq\ & c_2c_1\big(\|p-p_h\|_0\|p-p_h\|_1 + \|u-u_h\|_0\|u-u_h\|_1\big) \\ &+c_2c_1\big(\|u_h-u_H\|_0\|u_h-u_H\|_1 + \|p_h-p_H\|_0\|p_h-p_H\|_1\big) \end{aligned} \tag{4.15}$$

with $c_2 = \max\{1,\beta^{-1}\}$.

By a proper choice of the parameters of Young's inequality and Lemma 2.2, we have

$$\begin{aligned} \|p-p_h\|_0\|p-p_h\|_1 + \|u-u_h\|_0\|u-u_h\|_1 &\leq \tfrac{1}{2\sqrt{C_0}H^\gamma}(\|u-u_h\|_0^2 + \|p-p_h\|_0^2) \\ &\quad +\tfrac{\sqrt{C_0}H^\gamma}{2}(\|u-u_h\|_1^2 + \|p-p_h\|_1^2) \\ &\overset{(2.7)}{\leq} \sqrt{C_0}H^\gamma(|||u-u_h|||_e^2 + |||p-p_h|||_e^2) \end{aligned} \tag{4.16}$$

and

$$\begin{aligned} &\|u_h-u_H\|_0\|u_h-u_H\|_1 + \|p_h-p_H\|_0\|p_h-p_H\|_1 \\ \leq\ & \tfrac{\sqrt{2}}{4\sqrt{C_0}H^\gamma}(\|u_h-u_H\|_0^2 + \|p_h-p_H\|_0^2) \\ &+\tfrac{\sqrt{2C_0}H^\gamma}{2}(\|u_h-u_H\|_1^2 + \|p_h-p_H\|_1^2) \\ \leq\ & \tfrac{\sqrt{2}}{2\sqrt{C_0}H^\gamma}(\|u-u_H\|_0^2 + \|p-p_H\|_0^2) \\ &+\tfrac{\sqrt{2C_0}H^\gamma}{2}(\|u_h-u_H\|_1^2 + \|p_h-p_H\|_1^2) \\ \overset{(2.7)}{\leq}\ & \tfrac{\sqrt{2C_0}H^\gamma}{2}(|||u-u_H|||_e^2 + |||p-p_H|||_e^2) \\ &+\tfrac{\sqrt{2C_0}H^\gamma}{2}(\|u_h-u_H\|_1^2 + \|p_h-p_H\|_1^2). \end{aligned} \tag{4.17}$$

Then a collection of (4.14), (4.16) and (4.17) with $C_6 = \frac{c_1 c_2 \sqrt{2C_0}}{2}$ yields

$$\begin{aligned}(1-2C_6H^\gamma)(|||u-u_h|||_e^2+|||p-p_h|||_e^2) \quad &\leq \quad (1+C_6H^\gamma)(|||u-u_H|||_e^2+|||p-p_H|||_e^2)\\ &\quad -(1-C_6H^\gamma)(|||u_h-u_H|||_e^2+|||p_h-p_H|||_e^2).\end{aligned} \tag{4.18}$$

and

$$\begin{aligned}(1-C_6H^\gamma)(|||u-u_H|||_e^2+|||p-p_H|||_e^2) \quad &\leq \quad (1+2C_6H^\gamma)(|||u-u_h|||_e^2+|||p-p_h|||_e^2)\\ &\quad +(1+C_6H^\gamma)(|||u_h-u_H|||_e^2+|||p_h-p_H|||_e^2),\end{aligned} \tag{4.19}$$

which implies the desired result (4.12) and (4.13) immediately. □

5 Convergence of AFEM

In this section, we prove the convergence of the $\mathcal{AFEM}$ algorithm developed in Section 3 by showing the error reduction property with respect to the total error measure:

$$e_k + \mu\eta_k^2,$$

where $e_k := |||u-u_k|||_e^2 + |||p-p_k|||_e^2$ and μ is a positive constant to be determined in the subsequent analysis.

Based on the lemmas developed in Section 4, we are now in a position to state our first main theorem.

Theorem 5.1. *Let $\{T^k\}_{k\geq 0}$ be a sequence of meshes generated by algorithm $\mathcal{AFEM}$ and let $\{u_k, p_k\}_{k\geq 0}$ be the corresponding sequence of finite element solutions. Under the assumption that the mesh size h_{T^k} on T^k is small enough, there exist some $\mu > 0$ and $0 < \rho < 1$ such that for all $k = 1, 2, \ldots$*

$$e_{k+1} + \mu\eta_{k+1}^2 \leq \rho\,(e_k + \mu\eta_k^2). \tag{5.20}$$

Proof. First by letting T^H, T^h be T^k and T^{k+1}, respectively, using (4.12) of Lemma 4.5, (4.3) of Lemma 4.3, (3.16) and (4.1) of Lemma 4.1, we obtain

$$\begin{aligned}
& (1-2C_6h_{T^k}^\gamma)e_{k+1} + \mu\eta_{k+1}^2 \\
\overset{(4.12),(4.3)}{\leq} \quad & (1+C_6h_{T^k}^\gamma)e_k + \mu(1+\delta_1)\eta_k^2 - \tfrac{1}{2}\mu(1+\delta_1)\eta_k^2(\mathcal{F}^k) \\
& -(1-C_6h_{T^k}^\gamma - \mu C_3(1+\tfrac{1}{\delta_1}))(|||u_k-u_{k+1}|||_e^2 + |||p_k-p_{k+1}|||_e^2) \\
\overset{(3.16)}{\leq} \quad & (1+C_6h_{T^k}^\gamma)e_k + \mu(1+\delta_1)\eta_k^2 - \tfrac{1}{2}\mu(1+\delta_1)\theta\eta_k^2 \\
& -(1-C_6h_{T^k}^\gamma - \mu C_3(1+\tfrac{1}{\delta_1}))(|||u_k-u_{k+1}|||_e^2 + |||p_k-p_{k+1}|||_e^2) \\
= \quad & (1+C_6h_{T^k}^\gamma)e_k + \mu(1+\delta_1)(1-\tfrac{(1-b)\theta}{2})\eta_k^2 - \tfrac{\theta}{2}\mu(1+\delta_1)\eta_k^2 \\
& -(1-C_6h_{T^k}^\gamma - \mu C_3(1+\tfrac{1}{\delta_1}))(|||u_k-u_{k+1}|||_e^2 + |||p_k-p_{k+1}|||_e^2) \\
\overset{(4.1)}{\leq} \quad & (1+C_6h_{T^k}^\gamma - \tfrac{b\theta}{2C_1}\mu(1+\delta_1))e_k + \mu(1+\delta_1)(1-\tfrac{(1-b)\theta}{2})\eta_k^2 \\
& -(1-C_6h_{T^k}^\gamma - \mu C_3(1+\tfrac{1}{\delta_1}))(|||u_k-u_{k+1}|||_e^2 + |||p_k-p_{k+1}|||_e^2),
\end{aligned} \tag{5.21}$$

where the constant $b \in (0,1)$ is chosen in the following analysis.

If we choose μ and δ_1 such that

$$1 - C_6h_{T^k}^\gamma - \mu C_3(1+\frac{1}{\delta_1}) = 0, \tag{5.22}$$

the inequality (5.21) becomes

$$(1-2C_6h_{T^k}^{\gamma})e_{k+1}+\mu\eta_{k+1}^2 \quad \leq \quad (1+C_6h_{T^k}^{\gamma}-\tfrac{\theta}{2C_1}\mu(1+\delta_1))e_k+\mu(1+\delta_1)(1-\tfrac{(1-b)\theta}{2})\eta_k^2. \tag{5.23}$$

Then the desired result (5.20) will be obtained if there holds

$$\frac{b\theta}{2C_1}\mu(1+\delta_1) > 3C_6h_{T^k}^{\gamma} \tag{5.24}$$

and

$$(1+\delta_1)(1-\frac{(1-b)\theta}{2}) < 1. \tag{5.25}$$

The inequality (5.25) is equivalent to

$$(1-b) > \frac{2\delta_1}{(1+\delta_1)\theta}. \tag{5.26}$$

Thus if δ_1 is chosen such that

$$0 < \delta_1 < \frac{\theta}{2-\theta}, \tag{5.27}$$

then there exists a desired constant b according to (5.26). Lastly, when δ_1 and b are fixed, then μ can be chosen according to (5.22). Note that (5.24) is guaranteed if the mesh scale h_{T^k} is small enough. The proof is completed. □

6 Quasi-optimality and optimal complexity of AFEM

In this section, we establish the quasi-optimality and optimal complexity of $\mathcal{AFEM}$. In order to investigate the optimal complexity, we introduce some notations from nonlinear approximation theory, developed in [10, 11, 17]. Let $\mathcal{H}_N$ be the set of all triangulations T^h which satisfy $N_h \leq N$.

Next we define the approximation class

$$\mathcal{W}^s := \Big\{(u,p,f) \in (H^1(\Omega), H^1(\Omega), L^2(\Omega)) : \|(u,p,f)\|_{\mathcal{W}^s} < +\infty\Big\} \tag{6.28}$$

with

$$\|(u,p,f)\|_{\mathcal{W}^s} := \sup_{N\geq N_0} N^s \inf_{T^h\in\mathcal{H}_N}\Big(|||u-u_h|||_1^2+|||p-p_h|||_1^2+\mathrm{osc}_h^2\Big). \tag{6.29}$$

The infimum above means that T^h runs through all admissible triangulations that are refined by newest vertex bisection algorithm, satisfying $N_h \leq N$. The quasi-optimality of an adaptive finite element method is meant that whenever $(u,p,f) \in \mathcal{W}^s$, it produces a triangulation T^k with cardinal number N_k and corresponding approximation (u_k, p_k) such that

$$e_k^2+\eta_k^2 \leq C(N_k-N_0)^{-s}. \tag{6.30}$$

Our second main theorem is devoted to show $\mathcal{AFEM}$ enjoys a quasi-optimal convergence rate for the inverse problem.

Theorem 6.1. *Let $\{T^k\}_{k\geq 0}$ be a sequence of meshes generated by algorithm $\mathcal{AFEM}$ and let $\{u_k,p_k\}_{k\geq 0}$ be the corresponding sequence of finite element solutions. Under the assumption that h_{T^k} is small enough and*

$$0 < \theta < \theta^* \tag{6.31}$$

with

$$\theta^* := \frac{1 - C_1C_2C_4h_{T^k}^{2\gamma}\left(\frac{1+C_6h_{T^k}^{\gamma}}{1-C_6h_{T^k}^{\gamma}} + C_3^*\right)}{C_2C_4\left(\frac{1+C_6h_{T^k}^{\gamma}}{1-C_6h_{T^k}^{\gamma}} + C_3^*\right) + C_2},$$

then there exists a constant C such that for all $k = 1, 2, \ldots$

$$e_k^2 + \mu\eta_k^2 \leq C\left(N_k - N_0\right)^{-s}. \tag{6.32}$$

Proof. We suppose $\lambda \in (0, 1)$ is a constant to be chosen appropriately below and according to the definition of the $\mathcal{W}^s$ norm, there exists an admissible mesh T^{h^*} with the edge set $\mathcal{F}^{h^*}$, which is refined from T^0 with minimum number of elements such that

$$|||u - u_{h^*}|||_e^2 + |||p - p_{h^*}|||_e^2 + \mathrm{osc}_{h^*}^2(u_{h^*}, p_{h^*}) \leq \lambda(e_k^2 + \mu\eta_k^2) \tag{6.33}$$

with

$$N_{h^*} \leq \lambda^{-1/s}(e_k^2 + \mu\eta_k^2)^{-1/s}\|(u, p, f)\|_{\mathcal{W}^s}^{1/s}. \tag{6.34}$$

Next we choose $T^{h'}$ (with the edge set $\mathcal{F}^{h'}$) as the refinement of T^k with minimal number of elements such that $T^{h'} \subset T^{h^*}$ and thus

$$\begin{array}{rcl} |||u - u_{h'}|||_e^2 + |||p - p_{h'}|||_e^2 + \mathrm{osc}_{h'}^2(u_{h'}, p_{h'}) & \leq & (|||u - u_{h^*}|||_e^2 + |||p - p_{h^*}|||_e^2 + \mathrm{osc}_{h^*}^2(u_{h^*}, p_{h^*})) \\ & \leq & \lambda(e_k^2 + \mu\eta_k^2). \end{array} \tag{6.35}$$

Since both the triangulations $T^{h'}$ and T^k are refinements of T^0 and the former can be obtained from the latter by using at most $N_{T^{h'}}$ refinements (cf. [33]). Therefore by the property of newest vertex bisection in Lemma 2.2, there holds

$$N_{T_{h'}} - N_k \leq C_0^* N_{h^*} \leq C_0^*\lambda^{-1/s}(e_k^2 + \mu\eta_k^2)^{-1/s}\|(u, p, f)\|_{\mathcal{W}^s}^{1/s}. \tag{6.36}$$

In the following we will bound $N_{k+1} - N_k$ by $N_{T_{h'}} - N_k$ to obtain the desired results. In view of Lemma 4.4, there exists a subset $\mathcal{F}^{h^*} = F^k \backslash (F^k \cap F^{h'}) \subset F^k$ such that

$$|||u_k - u_{h'}|||_e^2 + |||p_k - p_{h'}|||_e^2 \leq C_4(\eta_k^2(\mathcal{F}^{h^*} + h_{T_k}^{2\gamma}e_k^2) \tag{6.37}$$

and

$$N_{\mathcal{F}^{h^*}} \leq C_5(N_{T_{h'}} - N_k). \tag{6.38}$$

On the other hand, if we choose λ such that

$$0 < \lambda < \frac{1}{2}.$$

From Lemma 4.1, Lemma 4.2, the second inequality in Lemma 4.3, Lemma 4.4, the second inequality in Lemma 4.5, and the fact that

$$\mathrm{osc}_k^2(u_k, p_k, \mathcal{F}^{h^*}) \leq \eta_k^2(\mathcal{F}^{h^*}) \tag{6.39}$$

together with (6.35), we obtain

$$
\begin{aligned}
(1-2C^*\lambda)\eta_k^2 &\overset{(4.2)}{\leq} C_2(1-2\lambda)(e_k^2+\mathrm{osc}_k^2(u_k,p_k))\\
&\overset{(6.35)}{\leq} C_2\Big(e_k^2-2(|||u-u_{h'}|||_e^2+|||p-p_{h'}|||_e^2)+\mathrm{osc}_k^2(u_k,p_k)-2\mathrm{osc}_{h'}^2(u_{h'},p_{h'})\Big)\\
&\leq C_2\Big(e_k^2-\tfrac{1+2C_6h_{T^k}^\gamma}{1-C_6h_{T^k}^\gamma}(|||u-u_{h'}|||_e^2+|||p-p_{h'}|||_e^2)+\mathrm{osc}_k^2(u_k,p_k)-2\mathrm{osc}_{h'}^2(u_{h'},p_{h'})\Big)\\
&\overset{(4.13)}{\leq} C_2\Big(\tfrac{1+C_6h_{T^k}^\gamma}{1-C_6h_{T^k}^\gamma}(|||u_k-u_{h'}|||_e^2+|||p_k-p_{h'}|||_e^2)+\mathrm{osc}_k^2(u_k,p_k)-2\mathrm{osc}_{h'}^2(u_{h'},p_{h'})\Big)\\
&\leq C_2\Big(\tfrac{1+C_6h_{T^k}^\gamma}{1-C_6h_{T^k}^\gamma}(|||u_k-u_{h'}|||_e^2+|||p_k-p_{h'}|||_e^2)\\
&\quad+\mathrm{osc}_k^2(u_k,p_k,\mathcal{F}^{h^*})+\mathrm{osc}_k^2(u_k,p_k,T^k\cap T^{h'})-2\mathrm{osc}_{h'}^2(u_{h'},p_{h'},T^k\cap T^{h'})\big)\Big)\\
&\overset{(4.4),(6.39)}{\leq} C_2\Big(\Big(\tfrac{1+C_6h_{T^k}^\gamma}{1-C_6h_{T^k}^\gamma}+C_3^*\Big)(|||u_k-u_{h'}|||_e^2+|||p_k-p_{h'}|||_e^2)+\eta_k^2(\mathcal{F}^{h^*})\Big)\\
&\overset{(4.5)}{\leq} C_2\Big(C_4\Big(\tfrac{1+C_6h_{T^k}^\gamma}{1-C_6h_{T^k}^\gamma}+C_3^*\Big)(\eta_k^2(\mathcal{F}^{h^*})+h_{T^k}^{2\gamma}e_k^2)+\eta_k^2(\mathcal{F}^{h^*})\Big)\\
&\overset{(4.1)}{\leq} C_2\Big(C_4\Big(\tfrac{1+C_6h_{T^k}^\gamma}{1-C_6h_{T^k}^\gamma}+C_3^*\Big)(\eta_k^2(\mathcal{F}^{h^*})+C_1h_{T^k}^{2\gamma}\eta_k^2)+\eta_k^2(\mathcal{F}^{h^*})\Big),
\end{aligned}
\tag{6.40}
$$

where we have made the assumption that $\frac{1+2C_6h_{T^k}^\gamma}{1-C_6h_{T^k}^\gamma}\leq 2$, which only requires $h_{T^k}\leq(4C_6)^{\frac{1}{\gamma}}$.

It yields from (6.40)

$$
\eta_k^2(\mathcal{F}^{k^*})\geq\frac{(1-2\lambda)+C_1C_2C_4h_{T^k}^{2\gamma}\Big(\frac{1+C_6h_{T^k}^\gamma}{1-C_6h_{T^k}^\gamma}+C_3^*\Big)}{C_2C_4\Big(\frac{1+C_6h_{T^k}^\gamma}{1-C_6h_{T^k}^\gamma}+C_3^*\Big)+C_2}\eta_k^2. \tag{6.41}
$$

Therefore, if we choose λ such that

$$
0<\lambda\leq\frac{1-\theta\Big(C_2C_4\Big(\frac{1+C_6h_{T^k}^\gamma}{1-C_6h_{T^k}^\gamma}+C_3^*\Big)+C_2\Big)-C_1C_2C_4h_{T^k}^{2\gamma}\Big(\frac{1+C_6h_{T^k}^\gamma}{1-C_6h_{T^k}^\gamma}+C_3^*\Big)}{2}, \tag{6.42}
$$

which is possible due to (6.31), we have

$$
\eta_k^2(\mathcal{F}^{h^*})\geq\theta\eta_k^2. \tag{6.43}
$$

Since in the marking strategy we choose the minimal edge set $\mathcal{F}^k\subset F^k$ such that (3.16) holds, then we conclude that

$$
\begin{aligned}
N_{k+1}-N_k &\leq C_0^*N(\mathcal{F}^k)\leq C_0^*N(\mathcal{F}^{h^*})\\
&\leq C_0^*C_5(N_{T_{h'}}-N_k)\\
&\leq (C_0^*)^2C_5\lambda^{-1/s}(e_k^2+\mu\eta_k^2)^{-1/s}\|(u,p,f)\|_{\mathcal{W}^s}^{1/s}.
\end{aligned}
\tag{6.44}
$$

By Theorem 5.1, we finally deduce that

$$
\begin{aligned}
N_k-N_0 &= \sum_{i=0}^{k-1}(N_{i+1}-N_i)C_0^*\\
&\leq (C_0^*)^2C_5\lambda^{-1/s}\sum_{i=0}^{k-1}(e_i^2+\mu\eta_i^2)^{-1/s}\|(u,p,f)\|_{\mathcal{W}^s}^{1/s}\\
&\leq (C_0^*)^2C_5\lambda^{-1/s}\Big(\sum_{i=0}^{k-1}\rho^{\frac{k-i}{s}}\Big)(e_k^2+\mu\eta_k^2)^{-1/s}\|(u,p,f)\|_{\mathcal{W}^s}^{1/s}\\
&\leq (C_0^*)^2C_5\lambda^{-1/s}\tfrac{1-\rho^{\frac{k}{s}}}{1-\rho^{\frac{1}{s}}}(e_k^2+\mu\eta_k^2)^{-1/s}\|(u,p,f)\|_{\mathcal{W}^s}^{1/s},
\end{aligned}
\tag{6.45}
$$

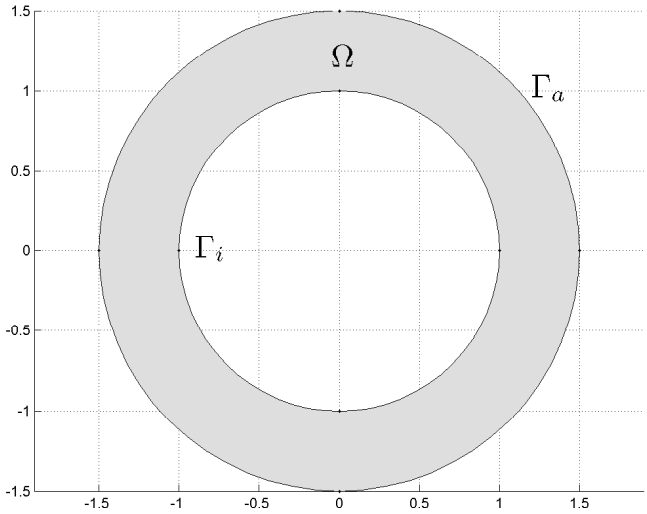

Figure 1: Computational domain for experiments.

which implies the desired result. The proof of the theorem is completed. □

It is remarked that the smallness assumption on h_{T^k} is essential in the proof of quasi-optimality of the $\mathcal{AFEM}$. One may refer to [33] for a nontrivial proof for an elliptic model problem for technical details.

As a direct corollary of Theorem 6.1, we obtain the following quasi-optimal complexity of the proposed adaptive algorithm.

Corollary 6.2. *Under the same assumptions of Theorem 6.1, there exists a constant C such that for all $k = 1, 2, \ldots$, such that the following estimate on the complexity of the algorithm holds:*

$$N_k - N_0 \leq C \left(e_k^2 + \mu\eta_k^2\right)^{-\frac{1}{s}}. \tag{6.46}$$

7 Numerical results and discussions

In this section we report two numerical experiments to validate the convergence and optimality of the proposed adaptive algorithm. Throughout the section, the spatial discretization is always done with continuous piecewise linear finite elements on triangles. The resulting discrete optimality system (2.6) are treated by fast direct solvers in the UMFPACK library. All the computations are done using Matlab and C++ compiler on a eight-core linux destop with AMD 925 processors and 16GB memory.

The computational examples arise from an application in steel furnace. For the tests, the computational domain is chosen to be a concentric disk with radii 1 and 1.5, respectively, as shown in Figure 1. For ease of visualization, the inner boundary plot of the flux is parametrized by its arc length (in the angular direction $[-\pi, \pi]$) so that both the exact and constructed fluxes can be represented by a function of arc length in one dimension.

In the sequel, the simulated noisy data is synthesized as follows:

$$z(x) = u(x) + \delta \cdot u(x)\mathrm{rand}(x)$$

where $u(x)$ denotes the true solution, δ represents the noise level and $\mathrm{rand}(x)$ is a nodal-wise uniformly random number between -1 and 1. For parameters, we set $\alpha = 1$, $k = 1$, $u_a = 0$ and $f = 0$. The noise level δ is always chosen to be 1%. The regularization parameter β is obtained by trial and error,

ranging from 10^{-4} to 10^{-7}. The initial guess of the unknown flux is always set to zero everywhere. The parameter θ in the marking strategy is chosen to be 0.6. To satisfy the assumption of fineness of the initial mesh, we start with an initial mesh of about 2400 DOF's and mesh size 0.1.

Example 1. (Discontinuous flux) The *exact* flux to be constructed is discontinuous at the points $(0,1)$ and $(0,-1)$ and given by the 2-D function

$$q_{exact}(x,y) = \begin{cases} 1 & \text{if } x > 0; \\ -1 & \text{if } x <= 0, \end{cases}$$

restricted on the inner boundary Γ_i.

The true solution u is shown in Figure 2(a). After 15 adaptive refinements from the initial mesh with 2400 DOF's, the adaptively refined mesh is shown in Figure 2(b). Local feature of the unknown flux is approximated reasonably well, see Figure 2(c). The loci of discontinuity in the flux are well captured with some oscillations around. Our adaptive algorithm refines adaptively elements around the singular points $(0,1)$ and $(0,-1)$. It is emphasized that the unique flux associated with (2.6) differs from the *exact* one and is unknown in general. Although the *exact* fluxes are specified with formulae, while the unique *true* flux corresponding to the problem (2.6) is only a regularized approximation of the *exact* one, which is a distinct feature of inverse problems. The convergence history of the error estimator versus the DOF's of the finite element discretization is plotted in Figure 2(d), which shows convergence and asymptotically optimal complexity $O(N^{-1})$ of the adaptive algorithm, compared with the reference red line of first order decay.

Example 2. (Dipole-like flux) We try to construct a dipole-shaped flux, which is even more challenging. The exact flux has a sharp sign change at the point $(0,1)$ and given by the 2-D function

$$q_{exact}(x,y) = \begin{cases} \exp(-10(x^2+(y-1)^2)) & \text{if } x > 0; \\ -\exp(-10(x^2+(y-1)^2)) & \text{if } x < 0, \end{cases}$$

restricted on the inner boundary Γ_i. The flux given makes the true solution u has a sharp sign change at $(0,1)$ as shown in Figure 3(a). Figure 3(b) is the final mesh after 15 adaptive refinements. Taking into account the challenging feature of the dipole-like flux, the reconstructed flux in Figure 3(c) is a good approximation to the exact one. Local feature of the unknown flux is successfully resolved by our adaptive algorithm, which adaptively refine elements around the singular point $(0,1)$ as shown in Figures 3(b). It is observed that the reconstructed heat fluxes capture well the location and height and even the sharp sign change of the dipole flux except small shift of the tips of the dipole flux. It is worthnoting that the local feature of the flux in this example is highly nontrivial, which requires far more local refinements for better recovering the sharp sign change. Through the convergence test shown in Figure 3(d), our adaptive algorithm achieves convergence and asymptotically optimal complexity of order $O(N^{-1})$.

8 Conclusion

We have proposed a modified adaptive algorithm for the inverse problem of distributed flux reconstruction. The proof of the convergence and optimality is rigorously shown by using an a posteriori local upper bound and quasi-orthogonality of solutions on successively refined meshes, based on the a posteriori error estimates developed in [23]. The generalization to other inverse problems will be reported elsewhere.

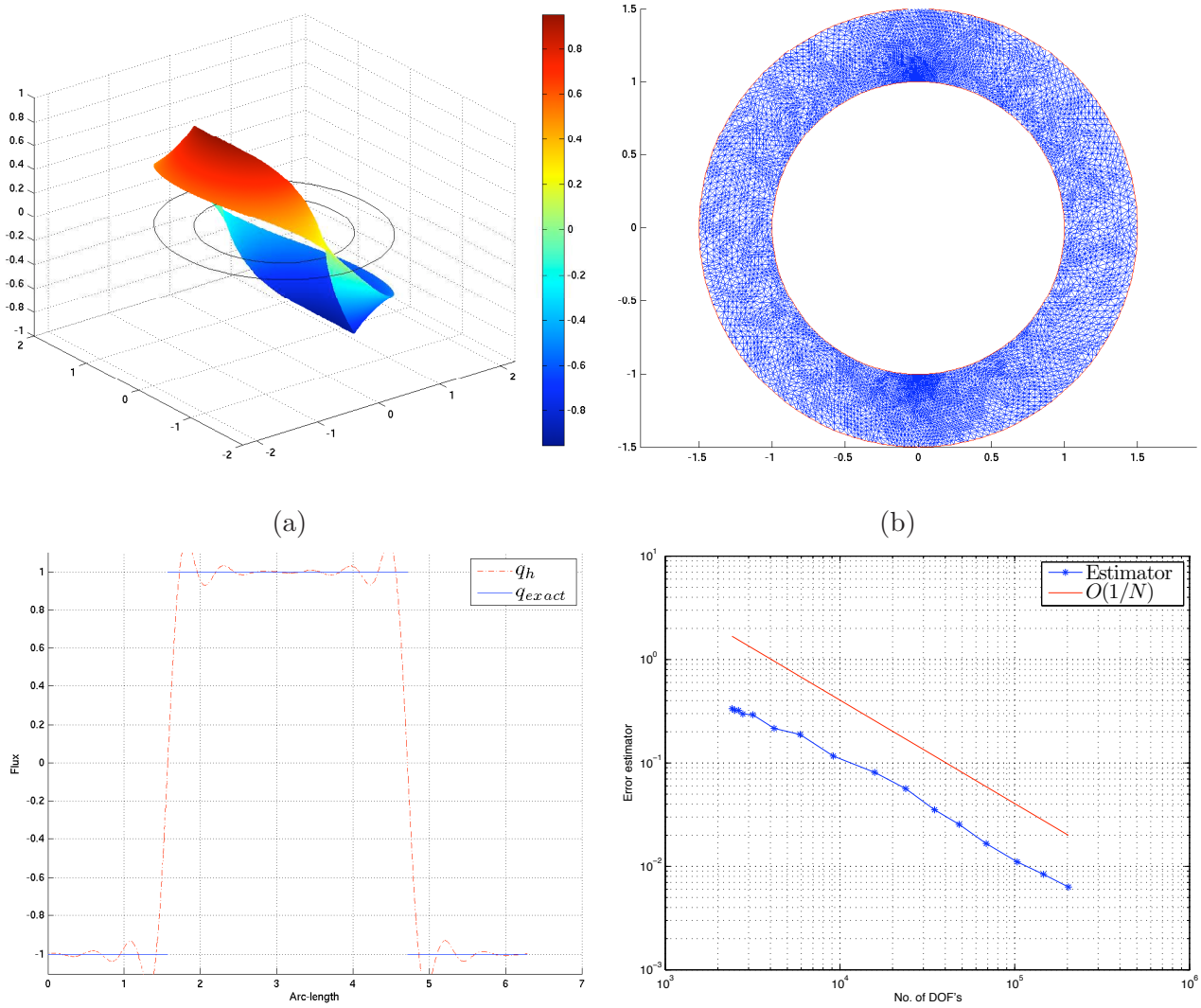

Figure 2: Example 1 : (a) True solution u, (b) and the final mesh with 203063 DOF's, (c) the reconstructed flux q_h with reference to the exact one q, and (d) global error indicator versus DOF's.

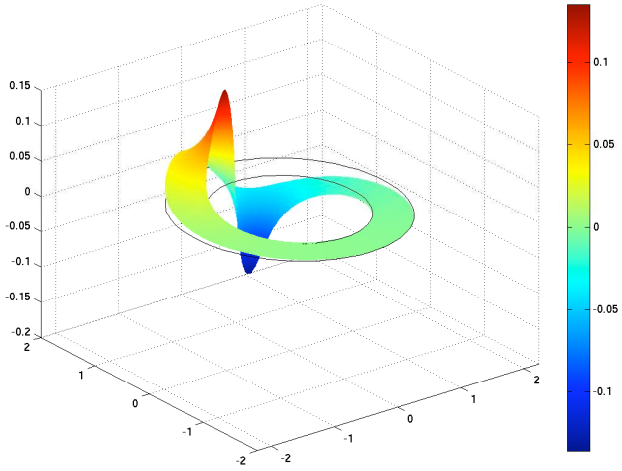

(a)

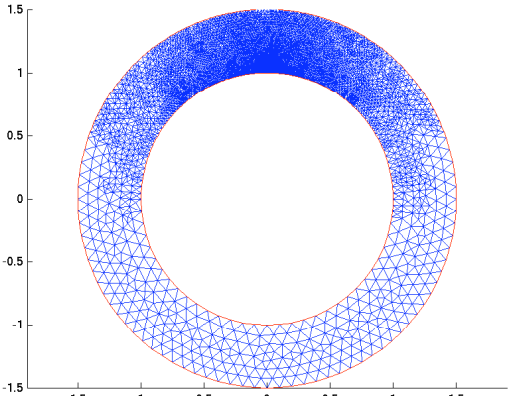

(b)

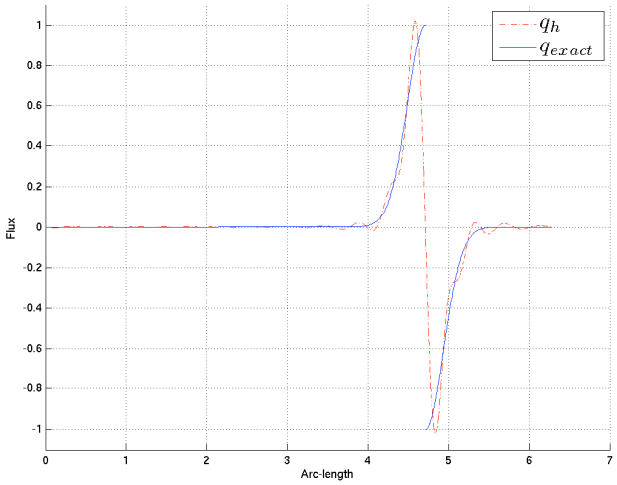

(c)

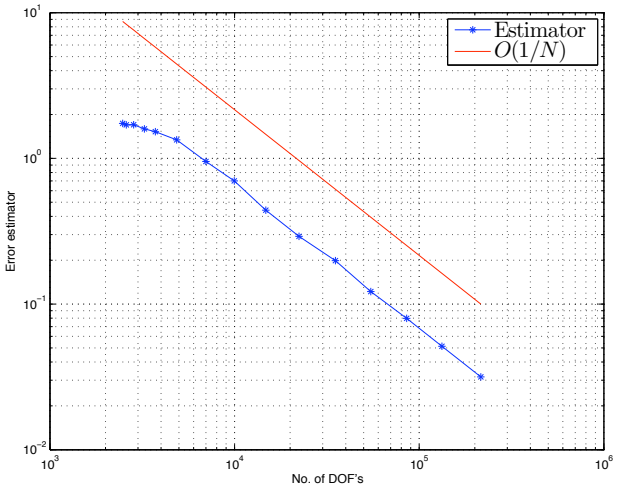

(d)

Figure 3: Example 2 : (a) True solution u, (b) and the final mesh with 215753 DOF's, (c) the reconstructed flux q_h with reference to the exact one q, and (d) global error indicator versus DOF's.

References

[1] O. M. Alifanov, Inverse Heat Transfer Problems. Springer: Berlin, 1994.

[2] I. Babuška and C. Rheinboldt, error estimates for adaptive finite element computations, SIAM J. Numer. Anal., 15 (1978), pp. 736–754.

[3] W. Bangerth and A. Joshi, Adaptive finite element methods for the solution of inverse problems in optical tomography, Inverse Problems, 24(3) (2008), pp. 1–22.

[4] R. Becker and B. Vexler, A posteriori error estimation for finite element discretization of parameter identification problems, Numer. Math., 96 (2004), pp. 435–459.

[5] R. Becker and S. Mao, An optimally convergent adaptive mixed finite element method, Numer. Math., 111(2008), 35-54.

[6] R. Becker and S. Mao, Convergence and quasi-optimal complexity of a simple adaptive finite element method, M2AN, 43 (2009), pp. 12031219.

[7] R. Becker, S. Mao, and Z.-C. Shi, A convergent nonconforming adaptive finite element method with optimal complexity, SIAM J Numer. Anal., 47(6), 2010, 4639-4659.

[8] R. Becker, S. Mao, Convergence of a simple adaptive finite element method for optimal control, Tech. report, Pau, 2008.

[9] L. Beilina and C. Johnson, A Posteriori Error Estimation in Computational Inverse Scattering, Math. Models Methods Appl. Sci., 15 (2005), pp. 23–35.

[10] P. Binev, W. Dahmen, and R. DeVore, Adaptive finite element methods with convergence rates., Numer. Math., 97 (2004), 219-268.

[11] P. Binev, W. Dahmen, R. DeVore, and P. Petruchev, Approximation classes for adaptive methods, Serdica Math. J., 28 (2002), 391-416.

[12] C. Carstensen and R. H. W. Hoppe, Convergence analysis of an adaptive nonconforming finite element methods, Numer. Math., 103(2006), 251-266.

[13] C. Carstensen and R. H. W. Hoppe, Error reduction and convergence for an adaptive mixed finite element method, Math. Comp., 75(2006), 1033-1042.

[14] J. M. Cascon, Ch. Kreuzer, R. H. Nochetto and K. G. Siebert, Quasi-optimal convergence rate for an adaptive finite element method, SIAM J. Numer. Anal. 46, (2008), 2524-2550.

[15] L. Chen, M. Holst, and J. Xu, Convergence and optimality of adaptive mixed finite element methods, Math. Comp., 78 (2009), pp. 35-53.

[16] P. G. Ciarlet, The Finite Element Method for Elliptic Problems, North-Holland, Amsterdam, 1978.

[17] R. DeVore, Nonlinear approximation., Acta Numerica 1998 (A. Iserles, ed.), vol. 7, Cambridege University Press, 1998, 51-150.

[18] E. Divo and J. S. Kapat, Multi-dimensional heat flux reconstruction using narrow-band thermochromic liquid crystal thermography, Inverse Problems in Science and Engineering, 9(5) (2001), pp. 537–559.

[19] W. Dörfler, A convergent adaptive algorithm for Poisson's equation., SIAM J. Numer. Anal. 33 (1996), 1106-1124.

[20] T. Feng, N. Yan, and W. Liu, Adaptive finite element methods for the identification of distributed parameters in elliptic equation, Adv. Comput. Math., 29 (2008), pp. 27-53.

[21] A. Gaevskaya, R. Hoppe, Y. Iliash, and M. Kieweg, Convergence analysis of an adaptive finite element method for distributed control problems with control constraints, In Control of Coupled Partial Differential Equations, Birkhäuser, Basel, 2007, pp. 47-68.

[22] J. Hadamard, Lectures on Cauchy's Problem in Linear Differential Equations. Yale University Press: New Haven, CT, 1923.

[23] J. Li, J. Xie, J. Zou, An adaptive finite element method for distributed heat flux reconstruction, to appear.

[24] M. Li, J. Li, S. Mao, L^2 error estimates of finite element method for distributed heat flux reconstruction, preprint.

[25] R. Li, W. Liu, H. Ma, and T. Tang, Adaptive finite element approximation for distributed elliptic optimal control problems, SIAM J. Control Optim., 41 (2002), pp. 1321–1349.

[26] W. Liu, H. Ma, T. Tang, and N. Yan, A posteriori error estimates for discontinuous galerkin time-stepping method for optimal control problems governed by parabolic equations, SIAM J. Numer. Anal., 42 (2004), pp. 1032–1061.

[27] W. Liu and N. Yan, A posteriori error estimates for optimal control problems governed by parabolic equations, Numer. Math., 93 (2003), pp. 497-521.

[28] K. Mekchay, R.H. Nochetto, Convergence of adaptive finite element methods for general second order linear elliptic PDE, SIAM J. Numer. Anal., 43(2005), 1803-1827.

[29] W. F. Mitchell. A comparison of adaptive refinement techniques for elliptic problems. ACM Transactions on Mathematical Software (TOMS) archive, 15(1989),326-347.

[30] P. Morin, R. H. Nochetto, and K.G. Siebert, Data oscillation and convergence of adaptive fem, SIAM J. Numer. Anal. 38 (2000), 466-488.

[31] P. Morin, R.H. Nochetto, and K.G. Siebert, Convergence of adaptive finite element methods, SIAM Review, 44 (2002), 631-658.

[32] L. R. Scott and S. Zhang, Finite element interpolation of nonsmooth functions satisfying boundary conditions, Math. Comp., 54 (1990), pp. 483–493.

[33] R. Stevenson, Optimality of a standard adaptive finite element method, Foundations of Computational Mathematics **7** (2007), no. 2, 245–269.

[34] R. Stevenson, The completion of locally refined simplicial partitions created by bisection, Math. Comp. 77 (2008), 227-241.

[35] J. Xie and J. Zou, Numerical reconstruction of heat fluxes, SIAM J. Numer. Anal., 43 (2005), pp. 1504–1535.

[36] N. Zabaras and S. Kang, On the solution of an ill-posed inverse design solidification problem using minimization techniques in finite and infinite dimensional spaces. Int. J. Numer. Meth. Engng., 36 (1993), pp. 3973–3990.

[37] N. Zabaras and J. Liu, An analysis of two-dimensional linear inverse heat transfer problems using an integral method. Numer. Heat Transfer, 13 (1988), pp. 527–533.

Research Reports

No.	Authors/Title
11-62	*J. Li, M. Li and S. Mao* Convergence analysis of an adaptive finite element method for distributed flux reconstruction
11-61	*J. Li, M. Li and S. Mao* A priori error estimates of a finite element method for distributed flux reconstruction
11-60	*H. Heumann and R. Hiptmair* Refined convergence theory for semi-Lagrangian schemes for pure advection
11-59	*V.A. Hoang and Ch. Schwab* N-term Galerkin Wiener chaos approximations of elliptic PDEs with lognormal Gaussian random inputs
11-58	*X. Claeys and R. Hiptmair* Electromagnetic scattering at composite objects: A novel multi-trace boundary integral formulation
11-57	*S. Mishra and L.V. Spinolo* Accurate numerical schemes for approximating intitial-boundary value problems for systems of conservation law
11-56	*P. Grohs* Finite elements of arbitrary order and quasiinterpolation for data in Riemannian manifolds
11-55	*P. Grohs* Bandlimited shearlet-type frames with nice duals
11-54	*A. Kunoth and Ch. Schwab* Analytic regularity and GPC approximation for control problems constrained by linear parametric elliptic and parabolic PDEs
11-53	*Ch. Schwab and S.A. Tokareva* High order approximation of probabilistic shock profiles in hyperbolic conservation laws with uncertain initial data
11-52	*F.Y. Kuo, Ch. Schwab and I.H. Sloan* Quasi-Monte Carlo finite element methods for a class of elliptic partial differential equations with random coefficients
11-51	*A. Chernov and Ch. Schwab* First order k-th moment finite element analysis of nonlinear operator equations with stochastic data
11-50	*E. Fonn* Shearlet Galerkin for transport equations: implementation and stability